COMPARING PER-PIXEL AND REGION-BASED CLASSIFICATION METHODS USING CBERS-4/MUX IMAGES TO ANALYSE LAND COVER CHANGE CAUSED BY THE MARIANA DISASTER

Daiane Vieira Vaz [1], Lucas Volochen Oldoni [1], Thales Sehn Körting [1], Leila Maria Garcia Fonseca [1], Ieda Del'Arco Sanches [1]

[1]Instituto Nacional de Pesquisas Espaciais – INPE, Caixa Postal 515 - 12227-010 - São José dos Campos - SP, Brasil
daiane.vaz@inpe.br; lucas.oldoni@inpe.br; thales.korting@inpe.br; leila.fonseca@inpe.br; ieda.sanches@inpe.br

ABSTRACT

In November 5th, 2015, the Fundão dam's rupture in Mariana, Minas Gerais, Brazil, dumped millions of cubic meters of tailing into the river, causing abrupt changes in the land cover (LC). Remote Sensing (RS) techniques and image analyses allow monitoring LC changes, that can contribute for decision making. In this paper we show results of LC change detection caused by the disaster applying per-pixel and region-based classifiers. For this purpose, three CBERS-4/MUX images were independently classified to assess LC in different periods: prior the incident, right after and its current situation. The per-pixel classification distinguished rivers from other classes, better than the region-based classification. In addition, the changes detected in the LC helped to highlight vegetation areas affected by the incident and also to evaluate its effects. Furthermore, the analysis was able to identify regenerated vegetation areas.

Key words — MUX, CBERS-4, Mariana Disaster, classification.

1. INTRODUCTION

In November 5th, 2015, the episode of a dam's rupture in the subdistrict of Bento Rodrigues, known as the disaster of Mariana, has probably been one of the biggest socio-environmental tragedies in Brazil. The Fundão dam was used with the purpose of depositing mining tailing. The tailing from the dam's rupture was dumped into the Doce River and its tributaries crossing 668 km to the Atlantic Ocean [1]. The amount of mud and iron waste directly affected 39 municipalities from both, state of Minas Gerais and Espírito Santo.

The destruction of the incident was enormous, people and animals died, houses and crops were destructed, and the water supply was compromised. The mud extended from about 1600 ha nearest the water bodies [2], completely changing the LC and the integrated ecosystems of the affected area. Since every living being depends of the natural LC of the Earth's surface, and the fact that its change along the time can reformulate ecosystems [3], the need of studies to detect and quantify LC changes is highlighted.

RS techniques are appropriate to detect LC changes, such as deforested areas, agriculture crops, urban growing, and also to provide information for environmental disasters. In this case, information derived from RS techniques contributes to the disaster's management and evaluation of the environmental impact, allowing risk assessment. It may help the decision makers to understand the consequences of these events, and propose mitigation acts [4].

Many authors have been applying classification techniques in order to detect and analyse LC change. Silva Junior et al. [4] quantified the land use changes caused by the Mariana disaster using the Unmixing Spectral Linear Model to separate vegetation, soil and shade and the Enhanced Vegetation Index (EVI) and the Normalized Difference Vegetation Index (NDVI) to evaluate vegetation changes.

Classification can be divided in per-pixel and region-based methods. The traditional per-pixel classification utilizes only spectral information [5], while region-based classifiers consider image segmentation and subsequent classification or object labelling. Segmentation identifies homogeneous regions and considers spectral reflectance variability as an attribute for discriminating features [6].

Thus, the objective of this work is to apply per-pixel and region-based classification techniques to evaluate the impact caused by the Mariana disaster in the LC, as well as to evaluate if changes in LC are taking place again with the regeneration of the vegetation.

2. MATERIAL AND METHODS

The study area extends for approximately 73 Km (kilometres), from the Fundão dam downstream to the rivers "Gualaxo do Norte" and "Do Carmo" (Fig. 1). In this study, a 500-meters buffer were created around these rivers in order to delimitate the areas to be analysed.

In order to analyse the LC change after the Mariana disaster CBERS-4 images acquired by MUX camera were used. The MUX sensor counts with four bands, B5, B6, B7 and B8, which respectively correspond to the spectral resolutions of 0.45-0.52 μm (blue), 0.52-0.59 μm (green), 0.63-0.69 μm (red), 0.77-0.89 μm (NIR - Near Infrared). The sensor's spatial resolution is 20 m, temporal resolution is 26 days and radiometric resolution is 8 bits. The images were obtained in the INPE's digital image catalogue [7].
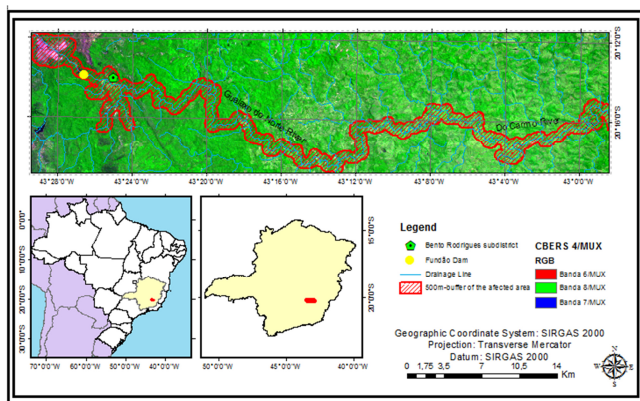
Figure 1. Location map of the studying area.

The methodology adopted in this paper is presented in Fig. 2. Three CBERS-4/MUX images were selected in the acquisition dates, 2015-10-04, 2016-02-11 and 2017-08-10. The criterion adopted for selecting these images was based on the low cloud-cover in the study area, and also on the proximity to the date in which the event occurred. These dates allowed to establish a scenario related to the situation before, shortly after and after the Mariana Disaster.
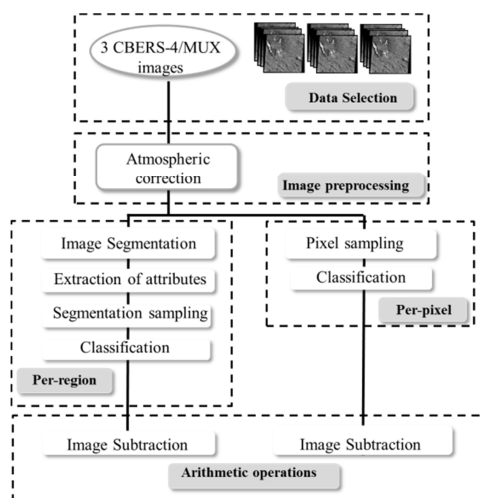

Figure 2. **Flowchart of the procedures performed.**

After data selection, the next step was to apply preprocessing operations. This stage was divided into two main phases: the transformation of the images to top of atmosphere reflectance images and the application of atmospheric correction [8]. The RS images were classified considering two classification approaches: a per-pixel classification, using Artificial Neural Networks (ANNs); and, a region-based classification, using a region-growing algorithm to segment the image and a decision tree classifier. The per-pixel classification procedures were developed using the ENVI software. The per-region

approach was carried out using the TerraView software and the GeoDMA plug-in [9].

The segmentation method used in the procedure is a region growing algorithm [10]. In this process, the algorithm considered a Euclidian distance and a minimum area of 50 and 20 pixels, respectively. These parameters were empirically chosen after performing several tests. In addition, training samples were collected in order to represent the following classes: soil (or sediments), vegetation and water. The samples acquisition was performed using the false-colour RGB composition, R: B6(green), G: B8(NIR), B: B7(red), in order to favour the targets identification. Table 1 shows the number of samples collected per class. Part of the samples (40%) was reserved to calculate the overall accuracy, as a validation method of the classifications.

Table 1. Number of collected samples.

Classification	Classes	Samples		
		2015-10-04	**2016-11-02**	**2017-08-10**
Per Pixel	**Vegetation**	865	1247	1152
	Water	162	107	240
	Soil	322	339	265
Per Region	**Vegetation**	178	80	45
	Soil	35	247	66

Finally, after classifying all the images using both classifiers, an arithmetic operation of subtraction was applied. The subtraction between the classification results produced from 2016-02-11 and 2015-10-04 images enables the identification of immediate changes caused by the disaster. In addition, it is possible to highlight areas of vegetation regeneration by applying the subtraction operation between the immediate changes result and the 2017-08-10 classified image. This process was independently performed to both classification results.

3. RESULTS AND DISCUSSION

Considering samples validation, the overall accuracy for per-pixel classifications was 99.48%, 98.93% and 99.27% for 2015-04-10, 2016-02-11 and 2017-08-10, respectively. The overall accuracy obtained for region-based classifications were 92.86%, 91.53%, 95.45% for the respective dates. Fig. 3 details an excerpt from the study area near the Fundão dam.

The per-pixel and per-region classification results showed a significant difference in the water class identification. The ANNs classifier was able to distinguish narrow river's stretches (Fig. 3a), better than the region-based classification algorithm (Fig. 3f). However, the per-pixel classifications (Fig. 3a, b and c) presented areas with isolated pixels, which does not occur in the per-region classifications (Fig. 3 f, g and h).
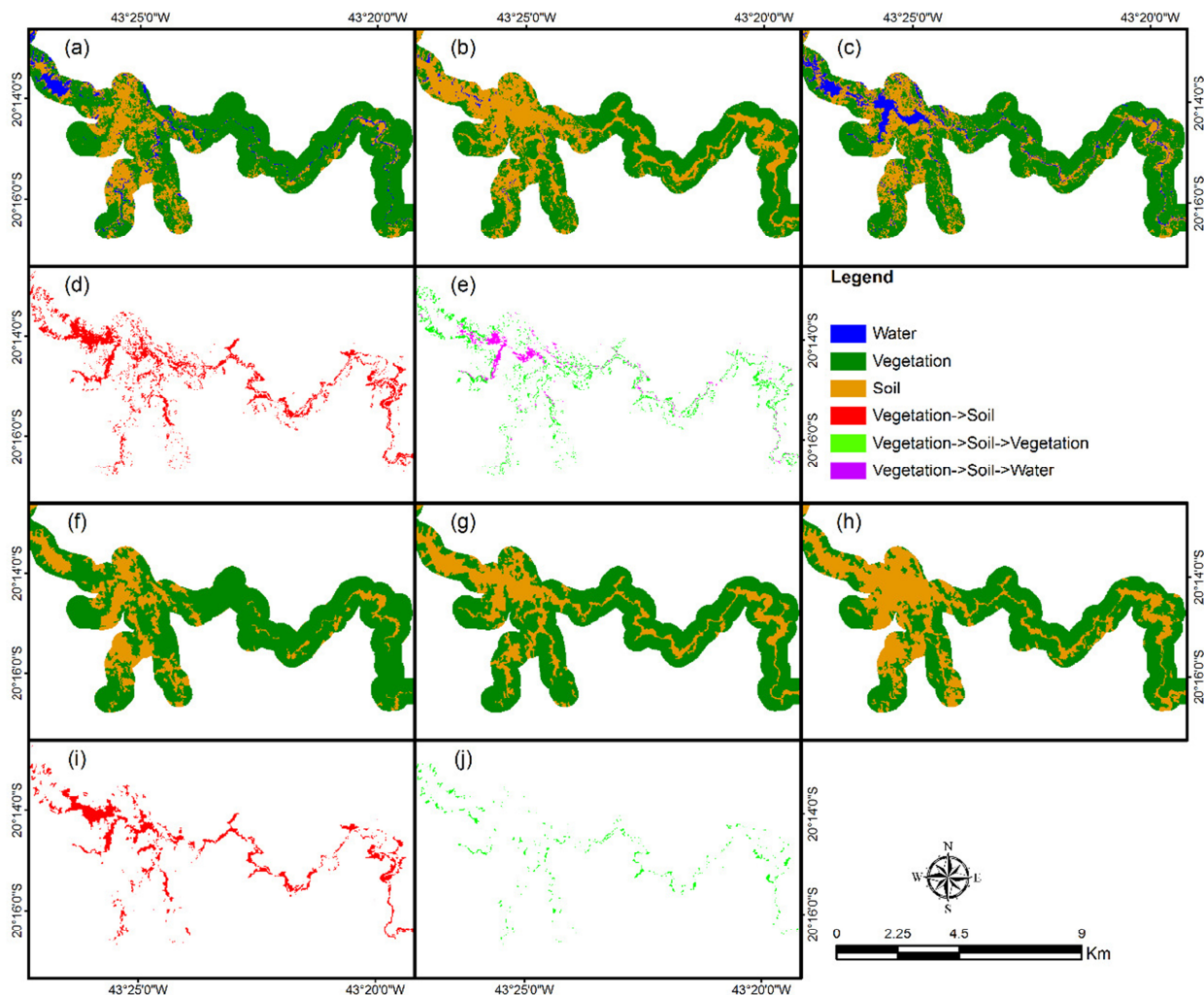
1832

Figure 3. Details of the per-pixel (a, b, c) and region-based classification (f, g, h) in near the Fundão dam area for previous (2015-10-04), posterior (2016-02-11) and recent (2017-08-10) images. Areas that changed from vegetation to soil with the disaster (d, i) and those affected areas that vegetation regenerated (e and j).

In both classification results of shortly after the disaster, the waterways weren't well distinguished from the soil's class. The entire Gualaxo do Norte River was classified as soil, and only part of the Do Carmo River was identified as water. This is probably due to the large amount of sediment in the river, which presents similar spectral response to the soil in the MUX spectral regions (visible and near infrared). Thus, both classifiers registered the enlargement of the soil's class (Fig. 3d and Fig 3i) due the riverside sediments gathering and the high presence of residue in water.

The 2017-08-10 image classifications identified some vegetation regeneration, highlighted in Fig. 3e and Fig 3j. In this case, the per-pixel result reveals some changes in the watercourses, as observed in Fig. 3e. Although after the disaster river stretches become wider, the region-based classifier still couldn't satisfactorily discriminate these rivers. Therefore, there is a greater number of areas that were affected by the disaster and then returned to being vegetation in the per-pixel classification.

Analysing the dynamics from pre to post-disaster, areas that changed from vegetation to soil were detected as 1430.3 ha (hectares) and 1311.5 ha, respectively by per-pixel and region-based classifications (Fig. 4). It occurred mainly due to the mud dumped into the river affecting the riverbed and banks (Fig. 3d and 3i). There also was a transition from soil to vegetation of 1803 ha and 1789 ha (Fig. 4) for per-pixel and region-based classifications, respectively. This change is attributed to the vegetation seasonality.

In the per-pixel classification, 780 ha changed from water class to soil class, between before and after disaster period, and 786 ha seem to have changed from soil to water from post-disaster to current date. River region classified as soil occurs due to the high sediment concentration, as discussed previously.
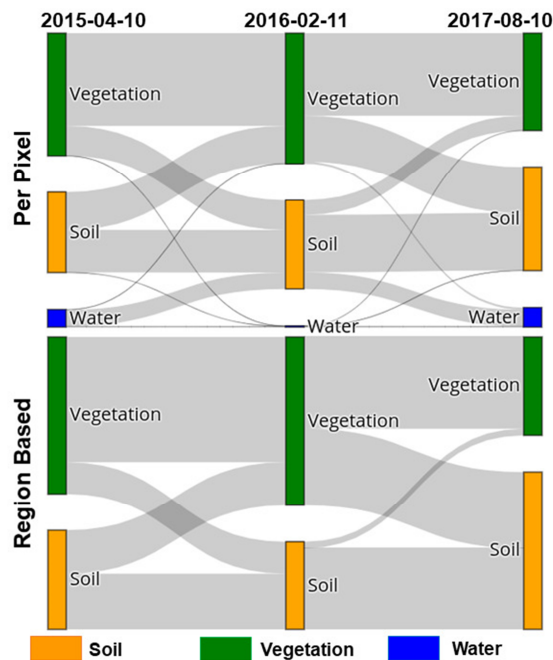
Figure 4. Sankey diagram for comparing the LC dynamics in three times intervals defined by LC maps produced by 015-10-04, 2016-02-11, 2017-08-10 images using the per-pixel and region-based classification.

A total of 707 ha changed from soil class to vegetation class, considering the per-pixel classification, from the post disaster picture to the recent image. Nonetheless, only 475 ha were vegetation (before scenery), then changed to soil (after), and returned to vegetation (current scenery). Evaluating the same situation, for the region-based classification, these values are lower. The total change from soil class to vegetation was 271 ha, but only 204 ha were identified from the areas affected by the sediment.

As shown in the Sankey diagrams, the per-pixel results gives more detail about the area dynamics. However, the isolated pixels can distort the results, which is probably what happened to the water portion that seems to change to vegetation and change back to water. The per-pixel classification also shows some small vegetation and soil areas that flooded shortly after the disaster and changed back to vegetation over time.

4. CONCLUSION

The use of per-pixel and region-based classification techniques in CBERS-4/MUX images enable the analysis and quantification of LC changes caused by the Mariana Disaster in the studying area. It shows that MUX images can be used in disaster monitoring. In the region-based classification results, it was not possible to differentiate the class water from the class soil for the study area. The number of classes and the waterways identification is limited due to CBERS-4/MUX images spatial resolution of 20 meters. In the post-disaster image it was also not possible to distinguish the river from the soil in areas affected by the mud as a result of the sediment load in water. To facilitate this discrimination it would be important to use spectral information of the studying area in the shortwave infrared.

5. ACKNOWLEDGEMENTS

6. REFERENCES

[1] Do Carmo, F.F.; Kamino, L.H.Y.; Junior, R.T.; De Campos, I.C.; Silvino, G.; et al, "Fundão tailings dam failures: the environment tragedy of the largest technological disaster of Brazilian mining in global context", 2017. In: Perspectives in Ecology and Conservation 15 (3), S. 145–151. DOI: 10.1016/j.pecon.2017.06.002.

[2] Prous, A., "Arquivos do Museu de História Natural e Jardim Botânico", UFMG Belo Horizonte. v. 24, n.1, 2015.

[3] Haque, M.I. and Basak, R., "Landcover change detection using GIS and remote sensing techniques: A spatio-temporal study on Tanguar Haor, Sunamganj, Bangladesh," Egypt. J. Remote Sens. Sp. Sci., vol. 20, no. 2, pp. 251–263, Dec. 2017.

[4] Silva Junior, C.A.; Coutinho, A.D.; de Oliveira-Júnior, J.F.; Teodoro, P.E.; Lima, M.; Shakir, M.; de Gois, G. and Johann, J.A., "Analysis of the impact on vegetation caused by abrupt deforestation via orbital sensor in the environmental disaster of Mariana, Brazil," Land use policy, vol. 76, no. March, pp. 10–20, Jul. 2018.

[5] Myint, S.W.; Gober, P.; Brazel, A.; Grossman-clarke, S. and Weng, Q., "Per-pixel vs. object-based classification of urban landcover extraction using high spatial resolution imagery," Remote Sens. Environ., vol. 115, no. 5, pp. 1145–1161, 2011.

[6] Johansen, K.; Bartolo, R. and Phinn, S., "SPECIAL FEATURE – Geographic Object-Based Image Analysis," J. Spat. Sci., vol. 55, no. 1, pp. 3–7, Jun. 2010.

[7] INPE – Instituto Nacional de Pesquisa Espacial. Catálogo de Imagens, http://www.dgi.inpe.br/CDSR (current Jul. 15, 2018).

[8] Da Silva, M.A.O.; Andrade, A.C., "Geração de Imagens de Reflectância de um Ponto de Vista Geométrico", Revista Brasileira de Geomorfologia, 2013;1(1):29-36.

[9] Körting, T.S.; Fonseca, L.M.G.; Câmara, G., "GeoDMA-Geographic Data Mining Analyst. Computer & Geosciences", 2013, 57:144-145. Available: http://linkinghub.elsevier.com/retrieve/pii/S0098300413000538.

[10] Bins, L.S.; Fonseca, L.M.G.; Erthal, G.J.; Ii, F.M., "Satellite imagery segmentation: a region growing approach", Simpósio Brasileiro de Sensoriamento Remoto, INPE, Salvador, 1996.